Shear-viscosity to entropy-density ratio from giant dipole resonances in hot nuclei

Nguyen Dinh Dang*

Theoretical Nuclear Physics Laboratory, RIKEN Nishina Center for Accelerator-Based Science, 2-1 Hirosawa, Wako City, 351-0198 Saitama, Japan and Institute for Nuclear Science and Technique, Hanoi, Vietnam

(Received 20 December 2010; revised manuscript received 17 June 2011; published 7 September 2011)

The Green-Kubo relation and fluctuation-dissipation theorem are employed to calculate the shear viscosity η of a finite hot nucleus directly from the width and energy of the giant dipole resonance (GDR) of this nucleus. The ratio η/s of shear viscosity η to entropy density s is extracted from the experimental systematics of the GDR in copper, tin, and lead isotopes at finite temperature T. These empirical results are then compared with the predictions by several independent models as well as with almost model-independent estimations. Based on these results, it is concluded that the ratio η/s in medium and heavy nuclei decreases with increasing temperature T to reach (1.3–4) $\times \hbar/(4\pi k_B)$ at $T = 5$ MeV.

DOI: 10.1103/PhysRevC.84.034309 PACS number(s): 24.10.Pa, 21.65.Mn, 24.30.Cz, 24.60.Ky

I. INTRODUCTION

The recent observations of the charged-particle elliptic flow and jet quenching in ultrarelativistic Au-Au and Pb-Pb collisions performed at the Relativistic Heavy Ion Collider (RHIC) [1] at Brookhaven National Laboratory and the Large Hadron Collider (LHC) [2] at CERN have been the key experimental discoveries in the creation and study of quark-gluon plasma (QGP). The analysis of the data obtained from the hot and dense system produced in these experiments revealed that the strongly interacting matter formed in these collisions is a nearly perfect fluid with extremely low viscosity. In the verification of the condition for applying hydrodynamics to a nuclear system, it turned out that the quantum-mechanical uncertainty principle requires a finite viscosity for any thermal fluid. In this respect, one of the most fascinating theoretical findings has been the conjecture by Kovtun, Son, and Starinets (KSS) [3] that the ratio η/s of shear viscosity η to the entropy volume density s is bounded below for all fluids, namely, the value,

$$\frac{\eta}{s} = \frac{\hbar}{4\pi k_B} \simeq 5.24 \times 10^{-23}\ \text{MeV s} \qquad (1)$$

is the universal lower bound (the so-called KSS bound or KSS unit). Although several theoretical counterexamples have been proposed, so far, no fluid that violates this lower bound has ever been found experimentally [4]. The QGP fluid produced at RHIC has $\eta/s \simeq$ (2 to 3) KSS units. Given this conjectured universality, there has been an increasing interest in calculating the ratio η/s in different systems.

The first theoretical study that calculated the ratio η/s for finite nuclei was the recent paper by Auerbach and Shlomo, who estimated $\eta/s =$ (4–19) and (2.5–12.5) KSS units for heavy and light nuclei, respectively [5]. These results were obtained within the framework of the Fermi-liquid-drop model (FLDM) [6], which was applied to the damping of giant collective vibrations. The calculated shear viscosity η in this paper increases with temperature T up to a quite high value of $T \sim 10$ MeV to reach a maximum at $T \sim 12$ to 13 MeV. At higher T, a decrease in η is seen. As a result, within the region $0 \leqslant T \leqslant 5$ MeV, where giant resonances exist, the damping width predicted by the FLDM always increases with T, which is roughly proportional to η [6,7]. Such temperature dependence contradicts the experimental systematics of the width of the giant dipole resonance (GDR) in hot nuclei. As a matter of fact, a large number of experiments on heavy ion fusion and inelastic scattering of light projectiles on heavy targets has shown that, while the location of the GDR peak (the GDR energy) is rather insensitive to the variation of T, its full width at half maximum (FWHM) increases with T only within $1 \leqslant T \leqslant 2.5$ MeV. Below $T \sim 1$ MeV, it remains nearly constant, whereas, at $T > 3$ to 4 MeV, the width seems to saturate [8–13]. To calculate the ratio η/s, the authors of Ref. [5] employed the Fermi-gas formula for the entropy $S = 2aT$ with a temperature-independent level-density parameter a. This approximation too is rather poor for finite nuclei, as has been pointed out by one of the authors of Ref. [5], who has proposed a fitting formula for the temperature-dependent density parameter $a(T)$ [14]. Therefore, although the ratio η/s, which was obtained in Ref. [5] by dividing two quantities that increase with T, does decrease qualitatively to reach a value within 1 order of the KSS bound as T increases up to $2 \sim 3$ MeV, it is highly desirable to obtain a refined quantitative estimation for this ratio in finite hot nuclei from both theoretical and experimental points of view.

The aim of the present paper is to calculate the ratio η/s directly from the most recent and accurate experimental systematics of the GDR widths in hot nuclei. The extracted empirical values are then confronted with theoretical predictions by four models, which have been developed to describe the temperature dependence of the GDR width, namely, the phonon-damping model (PDM) [15–17], two thermal-shape fluctuation models (TSFMs) [18,19], as well as the FLDM mentioned above. An attempt to pinpoint the high-temperature limit of the ratio η/s in finite nuclei in the most model-independent way is also undertaken.

The paper is organized as follows. The formalism of calculating the shear viscosity η from the GDR width and energy is discussed in Sec. II. The theoretical assessment

*dang@riken.jp

for the entropy density is given in Sec. III. The analysis of numerical results is presented in Sec. IV. The paper is summarized in the last section, where conclusions are drawn.

II. SHEAR VISCOSITY

A. Shear viscosity at zero temperature

The increase in widths of nuclear giant resonances by decreasing the mass number suggests that the damping mechanism of collective vibrations might qualitatively be similar to that of a viscous fluid, where damping of sound waves under the influence of viscosity increases as the system volume decreases [20]. From the viewpoint of collective theories, one of the fundamental explanations for the giant resonance damping remains the friction term (i.e., viscosity) of the neutron and proton fluids [7]. A quantitative description of the dissipative behavior requires an interparticle collision term to be included into the equation of motion for the one-body density matrix. For example, the nuclear-fluid-dynamics approach incorporated a collision term in the Landau-Vlasov equation to derive the momentum conservation, which includes three terms similar to the stress tensor, the shear modulus, and the dissipative component of the momentum flux tensor, respectively [6]. The latter resembles the viscous term in the macroscopic Navier-Stokes equation and is proportional to the damping coefficient of collective motion in the regime of rare collisions (zero-sound regime). Viscosity has also been employed to describe the decay of collective excitations in the context of nuclear fission in the 1970s [21].

In the microscopic description, the (quantal) width $\Gamma_Q(0)$ of giant resonances at $T = 0$ ($\sim$4 to 5 MeV in medium and heavy nuclei) consists of the Landau width Γ^{LD}, the spreading width $\Gamma^{\downarrow}$, and the escape width $\Gamma^{\uparrow}$. The Landau width Γ^{LD} is essentially the variance $\sigma = \sqrt{\langle E^2\rangle - \langle E\rangle^2}$ of the distribution of particle-hole (ph) states, which form the giant resonance. The spreading width $\Gamma^{\downarrow}$ is caused by coupling of $1p1h$ states to more complicated configurations, first of all, the $2p2h$ ones, whereas, the escape width $\Gamma^{\uparrow}$ arises because of coupling to the continuum causing the direct particle decay into hole states of the residual nucleus. In medium and heavy nuclei, Γ^{LD} and $\Gamma^{\uparrow}$ only account for a small fraction of the total width $\Gamma_Q(0)$. The major contribution is given by $\Gamma^{\downarrow}$. In light nuclei, $\Gamma^{\uparrow}$ gives a dominant contribution, whereas, Γ^{LD} is also mainly apparent. Within the semiclassical approaches, such as the Landau-Vlasov kinetic theory [22] or phenomenological approaches to nuclear friction [23], Γ^{LD} corresponds to the collisionless damping or one-body dissipation (long-mean-free path), whereas, $\Gamma^{\downarrow}$ comes from the collision damping or two-body dissipation (short-mean-free path). In the hydrodynamic theory of collective motion, which is based on a short-mean-free path, the dissipative effects are usually bulk phenomena caused by the viscous shearing stresses between adjacent layers of fluid. The microscopic mechanism of this energy dissipation resides in the coupling of $1p1h$ configurations to $2p2h$ ones, which causes the spreading width $\Gamma^{\downarrow}$ of giant resonances. This is how the shear viscosity is related to the damping of collective motion due to two-body interaction between nucleons in nuclei or molecules of a fluid.

The one-body dissipation (long-mean-free path) has been introduced based on the argument that the nucleon mean-free path is long compared to the nuclear radius. It arises primarily from the collisions of nucleons with the moving nuclear surface rather than with each other (the wall formula) [24]. Although neither the wall formula nor the ordinary two-body viscosity can correctly describe the experimental widths of giant resonances, the predictions by the two-body viscosity (short-mean-free path) are much closer to the experimental data [25]. As for the fission-fragment kinetic energies, the results obtained on the basis of one-body dissipation agree with the experimental values equally well as those predicted by two-body viscosity [26]. The evidence shows that a comprehensive view of the damping of giant resonances is likely a sum of one- and two-body contributions. This is consistent with the microscopic picture, where the one-body dissipation is described within the random-phase approximation (RPA), whereas, the two-body dissipation is taken into account by coupling the $1p1h$ states obtained within the RPA to $2p2h$ configurations or collective phonon beyond the RPA.

The discussion above indicates an uncertainty in extracting the value $\eta(0)$ of the shear viscosity $\eta(T)$ at $T = 0$, given different dissipation mechanisms. In Ref. [7], the two-body viscosity was employed under the assumption of a rigid nuclear boundary to fit the data of isovector and isoscalar giant resonances at $T = 0$. A value $\eta(0) \simeq 1u \simeq 0.016$ TP (terapoise) has been found, where $u = 10^{-23}$ MeV s fm^{-3}. The analysis of nuclear fission data based on the two-body collisions [26] gives $\eta(0)$ in the range of (0.6–1.2)u, or (0.01–0.02) TP, under the assumption that scission occurs at zero radius of the neck rupture. A later paper [27] assumed a finite radius for the neck rupture and found larger $\eta(0) = (1.1–2.5)u$ or (0.02–0.04) TP. The authors of Ref. [25] adopted $\eta(0) \simeq (1.9 \pm 0.6)u$, or 0.03 ± 0.01 TP, to calculate the widths of giant resonances for nuclei with deformable surfaces under the assumption of incompressible irrotational small-amplitude nuclear flow. The predicted theoretical widths are three times larger than the experimental values within the one-body dissipation mechanism based on the wall formula. For a modified one-body dissipation, the calculated widths are smaller than the experimental ones. In Ref. [28], the same authors calculated the fission-fragment kinetic energies using two-body viscosity in a similar way as that of Ref. [25] but with a modified potential. They found that the value $\eta(0) = 0.936u$ (0.015 TP) satisfactorily reproduces the experimental data. This value is very close to that obtained in Ref. [7]. The authors of Ref. [29] pointed out that anomaly large values of $\eta(0)$, in the range of (2–25)u, must be used to obtain a simultaneous description of the variances of mass distributions and multiplicities of prescission particles on the basis of both one- and two-body dissipations. The strong disagreement between the largest value $\eta(0) = 25u$ obtained in this case and those given in other references mentioned above sheds doubt on the possibility of consistently describing the mass-energy distribution and prescission-particle multiplicity.

In the present paper, the value $\eta(0) = 1u$, extracted in Ref. [7], is adopted as a parameter in combination with the lower and upper bounds, equal to $0.6u$ and $1.2u$, respectively, obtained in Ref. [26] and applied here as error bars. The

justification of this choice is based on two reasons. The first one is that the present paper considers the evolution of $\eta(T)$ as a function of T based on the GDR in hot-heavy (spherical or weakly deformed) nuclei. At $T = 0$, it should naturally be equal to $\eta(0)$ extracted from fitting the ground-state GDR (i.e., $T = 0$) in Ref. [7]. Moreover, according to Ref. [30], compact nuclei favor the two-body viscosity, whereas, the onset of one-body dissipation is seen only in fissioning nuclei when the necking in starts, which leads to a strong increase in the friction coefficient. This is also in line with the previously mentioned small contribution of Γ^{LD} and $\Gamma^{\uparrow}$ in heavy nuclei. The second reason is that the present paper attempts to see how low the ratio η/s can go with increasing T or how the KSS limit is fulfilled in hot nuclei. The lowest value of $\eta(0)$ found in the above-mentioned estimations is $\eta(0) = 0.6u$ [26]. The same lower bound has also been adopted in Ref. [5] to calculate $\eta(T)$ within the FLDM, where the upper bound varies within the range of $(1.9 \pm 0.6)u$, i.e., the same as used in Ref. [25]. As mentioned above, these large upper bounds fail to reproduce the giant resonance width.

B. Theoretical description of temperature dependence of shear viscosity $\eta(T)$

With these cautions regarding the selected values $\eta(0)$, one now proceeds to study the evolution of $\eta(T)$ as a function of T. The energy dissipation, which is a characteristic of a nonequilibrium or local thermodynamic equilibrium state (such as electrical conductivity, heat diffusion, shear viscosity,...) is related to fluctuations in statistical equilibrium or global thermodynamics equilibrium (such as thermal noise of electric and heat currents, collective vibrations,. . .) by means of the fluctuation-dissipation theorem (FDT) [31,32]. This is realized by making use of the Green-Kubo formula [33], which is an exact expression for the linear transport coefficient of any system at a given temperature T and density ρ in terms of the time dependence of equilibrium fluctuations in the conjugate flux. The Green-Kubo formula expresses the shear viscosity $\eta(T)$ in terms of the correlation function of the shear stress tensors $T_{xy}(t, \mathbf{x})$ as

$$\eta(T) = \lim_{\omega\to 0} \frac{1}{2\omega} \int dt\, d\mathbf{x}\, e^{i\omega t} \langle [T_{xy}(t, \mathbf{x}), T_{xy}(0, 0)]\rangle, \quad (2)$$

where the average $\langle\cdots\rangle$ is carried out within an equilibrium statistical ensemble, such as the grand canonical ensemble in the present paper. From the FDT, it follows that the integrated expression divided by 2ω on the right-hand side of Eq. (2) is proportional to the absorption cross section $\sigma(\omega, T)$. Therefore, the following identity holds:

$$\begin{aligned}\eta(T) &= \lim_{\omega\to 0} \frac{1}{2\omega i}[G_A(\omega) - G_R(\omega)] \\ &= -\lim_{\omega\to 0} \frac{\mathrm{Im}\, G_R(\omega)}{\omega} = \lim_{\omega\to 0} \frac{\sigma(\omega, T)}{C},\end{aligned} \quad (3)$$

where $G_A(\omega)$ and $G_R(\omega)$ are the advanced and retarded Green functions, respectively, with $G_R(\omega) = -i \int dt\, d\mathbf{x}\, e^{i\omega t}\theta(t)\langle [T_{xy}(t, \mathbf{x}), T_{xy}(0, 0)]\rangle$ and $G_A(\omega) = G_R(\omega)^*$. This relation has been employed in the anti-de Sitter/conformal field theory correspondence to derive the KSS conjecture [3], where C is equal to $16\pi G$ with G as the ten-dimensional gravitational constant. In Refs. [3,34], it has been shown that the graviton absorption cross section $\sigma(\omega)$, used on the right-hand side of Eq. (3), must not vanish in the zero-frequency limit ($\omega \to 0$) for nonextremal black branes, and is actually equal to the area of horizon so that one can use $\sigma(0)$ to obtain the shear viscosity of the hot supersymmetric Yang-Mills plasma. That Eqs. (2) and (3) indeed contain one-body dissipation has been shown, e.g., by the authors of Ref. [35], who derived the wall formula [24] as the small-frequency limit of the FDT.

In finite nuclei, the GDR photoabsorption cross section is quantum mechanically described by the Breit-Wigner distribution from the Breit-Wigner's theory of damping [36],

$$\begin{aligned}\sigma_{\mathrm{GDR}}(\omega) &= \sigma^{\mathrm{int}}_{\mathrm{GDR}} f^{\mathrm{BW}}(\omega, E_{\mathrm{GDR}}, \Gamma), \\ f^{\mathrm{BW}}(\omega, E_{\mathrm{GDR}}, \Gamma) &= \frac{1}{\pi} \frac{\Gamma/2}{[(\omega - E_{\mathrm{GDR}})^2 + (\Gamma/2)^2]},\end{aligned} \quad (4)$$

where $\sigma^{\mathrm{int}}_{\mathrm{GDR}} = (1 + k) \times \mathrm{TRK}$ is the GDR integrated cross section with the Thomas-Reiche-Kuhn (TRK) sum rule $\mathrm{TRK} = 60NZ/A$ (MeV mb), Γ is the FWHM of the GDR, and E_{GDR} is its energy. The enhancement factor $k \simeq 0.5$–0.7 represents the additional strength $k \times \mathrm{TRK}$ above the GDR and below the meson threshold at $\sim$140 MeV, which is usually attributed to the contribution caused by meson-exchange forces. By defining C as a normalization factor to reproduce the value $\eta(0)$ at $T = 0$ as

$$C = \frac{\lim_{\omega\to 0}[\sigma_{\mathrm{GDR}}(\omega, T = 0)]}{\eta(0)}, \quad (5)$$

and by inserting it as well as the right-hand side of Eq. (4) into that of Eq. (3), one obtains the final expression for the shear viscosity at temperature T in the form

$$\eta(T) = \eta(0)\frac{\Gamma(T)}{\Gamma(0)} \frac{E_{\mathrm{GDR}}(0)^2 + [\Gamma(0)/2]^2}{E_{\mathrm{GDR}}(T)^2 + [\Gamma(T)/2]^2}. \quad (6)$$

In principle, Eq. (6) is not limited to the GDR but can also be applied to calculate the temperature dependence of the transport coefficient in any transport process if its resonance scattering cross section is known. From Eq. (6), it is clear that, unlike the prediction by nuclear hydrodynamic theories (e.g., Ref. [6]), $\eta(T)$ is not proportional to the GDR width $\Gamma(T)$ but is an infinite geometric series of $x(T) \equiv \Gamma(T)/[2E_{\mathrm{GDR}}(T)]$, namely, $\eta(T) = \eta(0)[x(T)/x(0)][1 + x^2(0)] \sum_{n=0}^{\infty}(-)^n x^{2n}(T)$ $[x(T) < 1]$. It is proportional to $\Gamma(T)$ only in the limit of small damping ($x \ll 1$, the hydrodynamic regime), when Eq. (6) reduces to

$$\eta(T) \simeq \eta(0)\frac{\Gamma(T)}{\Gamma(0)}, \quad (7)$$

under the assumption that E_{GDR} does not depend on T. This limit can be verified independently by using the Stokes law of sound attenuation α, according to which, $\alpha = 2\eta\omega^2/(3\rho V^3)$. Indeed, by using the relation $\alpha = 2\Gamma(T)/v$, one obtains $\Gamma(T) = \eta(T)v\omega^2/(3\rho V^3)$. By knowing $\eta(0)$ and $\Gamma(0)$, one can determine $v = 3\rho V^3\Gamma(0)/[\eta(0)\omega^2]$. By inserting this expression of v into that of $\Gamma(T)$, one recovers the limit (7).

Because the GDR strength function in microscopic theories of the GDR damping is usually described with a single Breit-Wigner distribution or a superposition of them, in the present paper, Eq. (6) will be used to calculate the shear viscosity within the PDM and TSFM. It is worth mentioning that definition (5) avoids the necessity of requiring $\sigma(0, T) \neq 0$ because even with $\sigma(0, T) = 0$, inserting Eq. (5) into the right-hand side of Eq. (3) yields the 0/0-type limit for $\eta(T)$ (at $\omega \to 0$), which can be finite. This is actually the case, which is discussed later in Sec. II C, when the Lorentz distribution is used instead of the Breit-Wigner one (4) to fit the photoabsorption cross section.

Equation (6) shows that, given the values $\eta(0)$, the GDR width $\Gamma(T)$, and the energy $E_{\rm GDR}(T)$ at zero and finite T, one can calculate the shear viscosity $\eta(T)$ as a function of T. Considering the evolution of the GDR width as a function of T under the assumption that the microscopic mechanism of the quantal width of the GDR at $T = 0$ is known, the present paper adopts the predictions by four models, namely, the PDM [15–17], two versions of TSFM, namely, the adiabatic model (AM) [18] and the phenomenological parametrization of the TSFM (pTSFM) [19], and the FLDM [5,6]. Because these models have already been discussed in great detail in Refs. [5, 6,15–18], only their main features and/or results, used in the present paper, are summarized below.

1. PDM

The PDM employs a model Hamiltonian, which consists of the independent single-particle (quasiparticle) field, the GDR phonon field, and the coupling between them [See Eq. (1) in Ref. [15], for example]. The Woods-Saxon potentials for spherical nuclei at $T = 0$ are used to obtain the single-particle energies. These single-particle spectra span a large space from around -40 MeV up to around 17–20 MeV. They are kept unchanged with T based on the results of the temperature-dependent self-consistent Hartree-Fock calculations, which showed that the single-particle energies are not sensitive to the variation in T up to $T \sim 6$ to 7 MeV in medium and heavy nuclei [37]. The GDR width $\Gamma(T)$ is given as the sum of the quantal width $\Gamma_{\rm Q}$ and thermal width $\Gamma_{\rm T}$,

$$\Gamma(T) = \Gamma_{\rm Q} + \Gamma_{\rm T}. \tag{8}$$

In the presence of superfluid pairing, the quantal and thermal widths are given as [17]

$$\Gamma_{\rm Q} = 2\pi F_1^2 \sum_{ph} [u_{ph}^{(+)}]^2 (1 - n_p - n_h) \times \delta[E_{\rm GDR}(T) - E_p - E_h], \tag{9}$$

$$\Gamma_{\rm T} = 2\pi F_2^2 \sum_{s>s'} [v_{ss'}^{(-)}]^2 (n_{s'} - n_s) \times \delta[E_{\rm GDR}(T) - E_s + E_{s'}], \tag{10}$$

where (ss') stands for (pp') and (hh') with p and h denoting the orbital angular momenta j_p and j_h for particles and holes, respectively. Functions $u_{ph}^{(+)}$ and $v_{ss'}^{(-)}$ are combinations of the Bogoliubov coefficients u_j, v_j, namely, $u_{ph}^{(+)} = u_p v_h + v_p u_h$ and $v_{ss'}^{(-)} = u_s u_{s'} - v_s v_{s'}$. The quantal width is caused by coupling of the GDR vibration (phonon) to noncollective ph configurations with the factors $(1 - n_p - n_h)$, whereas, the thermal width arises because of coupling of the GDR phonon to pp and hh configurations, which includes the factors $(n_s - n_{s'})$ with $(s, s') = (h, h')$ or (p, p'). The quasiparticle occupation number n_j has the shape of a Fermi-Dirac distribution,

$$n_j^{\rm FD} = [\exp(E_j/T) + 1]^{-1} \tag{11}$$

smoothed with a Breit-Wigner kernel, whose width is equal to the quasiparticle damping with the quasiparticle energy $E_j = \sqrt{(\epsilon_j - \lambda)^2 + \Delta(T)^2}$ (see Eq. (2) of Ref. [17]). Here, ϵ_j, λ, and $\Delta(T)$ are the (neutron or proton) single-particle energy, the chemical potential, and the pairing gap, respectively. When the quasiparticle damping is small, as in the case for the GDR in medium and heavy nuclei, the Breit-Wigner-like kernel can be replaced with the δ function so that the quasiparticle occupation number n_j can be approximated with the Fermi-Dirac distribution $n_j \simeq n_j^{\rm FD}$ of noninteracting quasiparticles. The PDM predicts a slight decrease in the quantal width (in agreement with the finding that the Landau and spreading widths of the GDR do not change much with T [38]), a strong increase in the thermal width with increasing T, as well as a saturation of the total width at $T \geqslant 4$ to 5 MeV in tin and lead isotopes [15] in agreement with experimental systematics [8–13].

For the open-shell nuclei, the pairing parameters G are chosen for neutrons and/or protons to reproduce the empirical values at $T = 0$ for the neutron- and/or proton-pairing gaps $\Delta(0)$. In the presence of strong thermal fluctuations, the pairing gap $\Delta(T)$ of a finite nucleus does not collapse at the critical temperature T_c, which corresponds to the superfluid-normal phase transition predicted by the BCS theory for infinite systems, but decreases monotonically as T increases [39–42]. The effect caused by thermal fluctuations in quasiparticle numbers, which smooths out the superfluid-normal phase transition, is taken into account by using $\Delta(T)$ obtained as the solution of the modified BCS (MBCS) equations [40]. The use of the MBCS thermal-pairing gap $\Delta(T)$ for ^{120}Sn leads to a nearly constant GDR width or even a slightly decreasing one at $T \leqslant 1$ MeV [17] in agreement with the data of Ref. [11].

It is worth noticing that, within the PDM, the GDR strength function is calculated in terms of the GDR spectral intensity $J_q(\omega) = -2\,{\rm Im}[G_R(\omega)]/[\exp(\omega/T) - 1]$ with $G_R(\omega)$ as the retarded Green function associated with the GDR. Its final form reads

$$J_q(\omega) = f^{\rm BW}(\omega, \omega_q', 2\gamma_q)[e^{\omega/T} - 1]^{-1}, \tag{12}$$

with $\omega_q' = \omega_q + P_q(\omega)$, where ω_q is the unperturbed phonon energy, $P_q(\omega)$ is the polarization operator, which is arisen due to coupling of the GDR phonon to ph, pp, and hh configurations. The GDR energy is defined as the solution of the equation,

$$\omega - \omega_q - P_q(\omega) = 0, \tag{13}$$

at which, one obtains $\Gamma(T) = 2\gamma_q$ in Eq. (8). The use of Eq. (12) within the PDM then exactly yields Eq. (3). The PDM as well as the selection of its parameters F_1 and F_2 in Eqs. (9) and (10) are presented and are discussed thoroughly in Refs. [15–17] and references therein, to which the reader is referred for further details.

2. AM

The AM [18] assumes that the time scale for thermal fluctuations is slow compared to the shift of the dipole frequency caused by the fluctuations so that the GDR strength function can be averaged over all quadrupole shapes with deformation $\alpha_{2\mu}$ and orientations. The angular-momentum-projected GDR cross section $\sigma(\omega)$, at a given temperature T, is calculated within the AM as a thermal average over the shape-dependent cross sections $\sigma(\omega, \alpha_{2\mu}, \omega_J)$,

$$\sigma(\omega) = \frac{1}{Z_J}\int \frac{\mathcal{D}[\alpha]}{\mathcal{I}(\beta,\gamma,\theta,\psi)^{3/2}}\sigma(\omega,\alpha_{2\mu},\omega_J) \times \exp[-F(T,\alpha_{2\mu},\omega_J)/T], \quad (14)$$

where ω is the photon energy, $\mathcal{D}[\alpha] = \beta^4 \sin(3\gamma) d\beta\, d\gamma\, d\Omega$ is the volume element, $Z_J = \int \mathcal{D}[\alpha]\mathcal{I}^{-3/2}\exp[-F(T,\alpha_{2\mu},\omega_J)/T]$ is the partition function, $\mathcal{I}(\beta,\gamma,\theta,\psi) = I_1\cos^2\psi\sin^2\theta + I_2\sin^2\psi\,\sin^2\theta + I_3\cos^2\theta$ is the moment of inertia about the rotation axis, expressed in terms of the principal moments of inertia I_k and the Euler angle $\Omega = (\psi,\theta,\phi)$, and $F(T,\alpha_{2\mu},\omega_J) = F(T,\alpha_{2\mu},0) + (J+1/2)^2/[2\mathcal{I}(\beta,\gamma,\theta,\psi)]$ is the free energy with $F(T,\alpha_{2\mu},0)$ denoting the cranking free energy at $\omega_J = 0$. The free energy $F(T,\alpha_{2\mu},0)$ and the principal moments of inertia are calculated by using either the Nillson-Strutinsky approach, which includes shell corrections, or the liquid-drop model. The shape-dependent cross section $\sigma(\omega,\alpha_{2\mu},\omega_J)$ is calculated at the saddle-point frequency $\omega_J = (J+1/2)/\mathcal{I}(\beta,\gamma,\theta,\psi)$, where the GDR is approximated as a rotating three-dimensional oscillator, which consists of three fundamental modes with energies $E_k = 70\,A^{-1/3}\exp[-\sqrt{5/\pi}\beta\cos(\gamma + 2\pi k/3)/2]$ $(k = 1, 2, 3)$. The GDR Hamiltonian in the intrinsic frame is written as $H_{\rm GDR} = \sum_k (p_k^2 + E_k^2 d_k^2) + \vec{\omega}_{\rm rot}(\vec{d}\times\vec{p})$ where d_k and p_k are the coordinates and conjugate momenta of the GDR vibration and $\vec{\omega}_{\rm rot}$ is the rotation frequency. The GDR cross section in the intrinsic frame is calculated by using the Breit-Wigner distribution (4) as

$$\sigma(\omega,\alpha_{2\mu},\omega_J) = \sigma_0\sum_{\mu\nu}|\langle\nu|d_\mu|0\rangle|^2\omega[f^{\rm BW}(\omega,E_\nu,\Gamma_\nu) - f^{\rm BW}(\omega,-E_\nu,\Gamma_\nu)] = \sigma_0\sum_{\mu\nu}|\langle\nu|d_\mu|0\rangle|^2 E_\nu f^{\rm L}(\omega,E'_\nu,\Gamma_\nu), \quad (15)$$

where μ denote the spherical components of the dipole mode, $|\nu\rangle$ are the eigenstates of the model Hamiltonian, $\Gamma_\nu = \Gamma_0(E_\nu/E_0)^\delta$ $(\nu = 1, 2, 3)$ with $\delta = 1.8$ are the parametrized intrinsic widths of the three components of the GDR, which are centered at E_ν, whereas, E_0 and Γ_0, respectively, are the energy centroid and width of the GDR at $T = 0$. The function $f^{\rm L}(\omega, E'_\nu, \Gamma)$ is the Lorentz distribution,

$$f^{\rm L}(\omega,E'_\nu,\Gamma) = \frac{\omega}{E_\nu}[f^{\rm BW}(\omega,E_\nu,\Gamma) - f^{\rm BW}(\omega,-E_\nu,\Gamma)] = \frac{2}{\pi}\frac{\omega^2\Gamma}{[\omega^2-(E'_\nu)^2]^2+\omega^2\Gamma^2}, \quad (16)$$

with $(E'_\nu)^2 = E_\nu^2 + (\Gamma/2)^2$. The normalization factor σ_0 ensures the integrated cross section of the GDR to be equal to the TRK sum rule. The present paper uses the GDR widths obtained within the AM for ^{120}Sn and ^{208}Pb as shown by the solid lines in Fig. 1 of Ref. [18].

3. pTSFM

The pTSFM [19] is essentially a phenomenological parametrization of the AM discussed in the previous section. This model proposes a phenomenological fit for the width of a liquid-drop GDR as a function of temperature T, mass number A, and angular momentum J. For $J \leqslant 20\hbar$, as in the experimental systematics used in the present paper, this phenomenological fit reduces to

$$\Gamma(T,A) = \Gamma_0(A) + c(A)\ln\left(1+\frac{T}{T_0}\right), \qquad c(A) = 6.45 - A/100. \quad (17)$$

The reference temperature $T_0 = 1$ MeV is used in the pTSFM calculations. The present paper uses Eq. (17) to calculate the GDR width in copper, tin, and lead regions. The shell corrections within the Nillson-Strutinsky method are not included because they have almost no effect on the GDR width in open-shell nuclei, whereas, for lead isotopes, they are important only at $T \leqslant 1.2$ MeV as shown in Fig. 4 of Ref. [19].

4. FLDM

The FLDM employs a collision kinetic equation, which includes the dissipative propagation of a sound wave in infinite nuclear matter, to directly calculate the shear viscosity η as [5]

$$\eta(T) = \frac{2}{5}\rho\epsilon_{\rm F}\frac{\tau_{\rm coll}}{1+(\omega\tau_{\rm coll})^2}, \quad \tau_{\rm coll} = \frac{\tau_0}{1+(\hbar\omega/2\pi T)^2}, \quad \tau_0 = \hbar\alpha/T^2. \quad (18)$$

After inserting the explicit expressions for $\tau_{\rm coll}$ and τ_0, the expression for $\eta(T)$ becomes

$$\eta(T) = \frac{2}{5}\rho\epsilon_{\rm F}\frac{\hbar}{4\pi^2\alpha}\frac{1+(2\pi T/\hbar\omega)^2}{1+\{\hbar\omega[1+(2\pi T/\hbar\omega)^2]/(4\pi^2\alpha)\}^2}, \quad (19)$$

The calculations within the FLDM used the Fermi energy $\epsilon_{\rm F} = 40$ MeV and the nuclear density $\rho = 0.16$ fm^{-3} [5], whereas, the parameter α was estimated based on the in-medium-nucleon-nucleon scattering cross section to be between around 9.2 for isoscalar modes and 4.6 for the isovector ones [22]. The empirical giant resonance energy $\hbar\omega$ decreases from around 19 to 13 MeV as the mass number A increases from around

50 to 250 [43]. By adopting these values, one finds the factor $\{\hbar\omega/(4\pi^2\alpha)\}^2$ in the denominator of the expression on the right-hand side of Eq. (19) in the range between 0.001 and 0.01. This shows that $\eta(T)$ can be approximated at low T with the zero sound limit ($\omega\tau \gg 1,\ T \ll \hbar\omega$) as [5,6]

$$\eta(T)_{z.s} = \frac{2}{5}\rho\epsilon_{\rm F}\frac{\hbar}{4\pi^2\alpha}\left[1+\left(\frac{2\pi T}{\hbar\omega}\right)^2\right]. \tag{20}$$

By using this limit, one can also readjust the parameter α to reproduce the empirical values of $\eta(0) = 0.6u,\ 1.0u$, and $1.2u$, discussed previously in Sec. II A. This leads to $\alpha = 7.11$, 4.27, and 3.56, respectively. The lowest $\eta(0) \simeq 0.46u$ was obtained in Ref. [5] by using $\alpha = 9.2$.

The FLDM, however, only offers the expression for the collisional width but not for the FWHM of the GDR at $T \neq 0$ (See Eq. (333) of Ref. [6]) because it does not include the effect of collisionless damping (one-body dissipation). As a matter of fact, an attempt to fit this width with the total GDR width has resulted in a value of the cutoff factor $\bar{q}$, which is four times larger than the theoretically estimated realistic value $\bar{q} = 0.192$ [6]. With Eq. (6) proposed in the present paper, one can readily derive the FWHM $\Gamma(T)$ given the values of other parameters, namely, $r \equiv \eta(T)/\eta(0)$, $E_{\rm GDR}(T)$, $E_{\rm GDR}(0)$, and $\Gamma(0)$ by solving a simple quadratic equation for the unknown $\Gamma(T)$. As a result, one obtains

$$\Gamma(T) = \frac{4E_{\rm GDR}(0)^2 + \Gamma(0)^2 - \sqrt{[4E_{\rm GDR}(0)^2+\Gamma(0)^2]^2 - [4rE_{\rm GDR}(T)\Gamma(0)]^2}}{2r\Gamma(0)}. \tag{21}$$

The other solution (with the + sign in front of the square root) is excluded because it does not give $\Gamma(T) = \Gamma(0)$ at $T = 0$. To have a real value of $\Gamma(T)$ by Eq. (21), the expression under the square root in its right-hand side must not be negative. This leads to the constraint,

$$\frac{\eta(T)}{\eta(0)} \leqslant \frac{4E_{\rm GDR}(0)^2+\Gamma(0)^2}{4E_{\rm GDR}(T)\Gamma(0)}. \tag{22}$$

Based on the experimental systematics, which show that $E_{\rm GDR}(T)$ is not sensitive to the temperature change, one can set $E_{\rm GDR}(T) \simeq E_{\rm GDR}(0)$ in Eq. (22). By using the fit $\Gamma(0) \simeq 0.3E_{\rm GDR}(0)$ [7], from Eq. (22), it follows that

$$\frac{\eta(T)}{\eta(0)} \leqslant 3.41. \tag{23}$$

This means that, while one can calculate the shear viscosity $\eta(T)$ from the width and energy of the GDR from Eq. (6) at any T, the inverse is not true, that is, the GDR width $\Gamma(T)$, extracted from the same equation based on the values of shear viscosity $\eta(T)$ at zero and finite T as well as the values of $\Gamma(0)$ and $E_{\rm GDR}(0)$, breaks down to become imaginary at a temperature T_c, starting from which $\eta(T) > 3.41\eta(0)$. The width (21) also depends on $\eta(0)$, hence, on the parameter α, especially at high T when $2\pi T \sim \hbar\omega$, as can be inferred from Eq. (19).

C. Empirical extraction of shear viscosity $\eta(T)$ at $T \neq 0$

The experimental cross section of the GDR is often fitted with a Lorentz distribution $f^{\rm L}(\omega, E_{\rm GDR}, \Gamma)$, Eq. (16) [43] rather than with a Breit-Wigner one $f^{\rm BW}(\omega, E_{\rm GDR}, \Gamma)$, Eq. (4). The GDR energy in the Lorentz distribution (16) is defined as $E_{\rm GDR}^2 = E_D^2 + (\Gamma/2)^2$, where E_D is the energy of the dipole mode before switching on the coupling to configurations that cause the GDR width [44]. The nice fits obtained for a wide class of GDRs, built on the ground state ($T = 0$) of medium and heavy spherical nuclei, seem to justify such *ad hoc* practice. For the GDR at $T = 0$, one has $E_{\rm GDR} \gg 0$ and $\Gamma \ll E_{\rm GDR}$. Therefore, the Breit-Wigner component centered at $-E_D$ on the right-hand side of Eq. (16) for the Lorentz distribution has a negligible effect on the GDR shape and can safely be neglected, which leads to $f^{\rm L}(\omega, E_{\rm GDR}, \Gamma) \simeq (\omega/E_{\rm GDR})f^{\rm BW}(\omega, E_{\rm GDR}, \Gamma)$ with $E_{\rm GDR} \simeq E_D$. Differences arise when Γ becomes comparable with $E_{\rm GDR}$. Nonetheless, the Lorentz distribution has also been applied to fit the experimentally measured GDRs in hot nuclei where $\Gamma \sim E_{\rm GDR}$ at high T [8–13].

By using the Lorentz distribution $f^{\rm L}(\omega, E'_\nu, \Gamma)$, one has $\sigma(0, T) = 0$ because of the multiplier ω^2 on the right-hand side of Eq. (16), which vanishes at $\omega \to 0$. However, the definition of the normalization factor C by Eq. (5) guarantees the cancellation of this multiplier ω^2 in the expression for $\eta(T)$. Indeed, by dividing $\sigma(\omega, T)$ by the normalization factor C given by Eq. (5), and then by taking the limit $\omega \to 0$, one obtains the following expression for the shear viscosity:

$$\eta^{\rm L}(T) = \eta(0)\frac{\Gamma(T)}{\Gamma(0)}\left\{\frac{E_{\rm GDR}(0)^2}{E_{\rm GDR}(0)^2 - [\Gamma(0)/2]^2 + [\Gamma(T)/2]^2}\right\}^2. \tag{24}$$

In the present paper, to have an exhaustive comparison, both Eqs. (6) and (24) are used to extract the empirical shear viscosity from the experimental systematics of the GDR widths and energies obtained in hot nuclei.

III. ENTROPY DENSITY

The entropy density (entropy per volume V) is calculated as

$$s = \frac{S}{V} = \rho\frac{S}{A}, \tag{25}$$

with the nuclear density $\rho = 0.16\ \mathrm{fm}^{-3}$. The entropy S at temperature T is calculated by integrating the Clausius definition of entropy as

$$S = \int_0^T \frac{1}{\tau}\frac{\partial \mathcal{E}}{\partial \tau} d\tau, \tag{26}$$

where $\mathcal{E}$ is the total energy of the system at temperature τ, which is evaluated microscopically as within the PDM or macroscopically by using the Fermi-gas formula $\mathcal{E} = \mathcal{E}_0 + aT^2$ as within the FLDM.

By taking the thermal average of the PDM Hamiltonian and by applying Eq. (26), it follows that

$$S = S_F + S_B, \tag{27}$$

where S_F and S_B are the entropies of the quasiparticle and phonon fields, respectively (see Eq. (1) of Ref. [15]). The entropy S_α ($\alpha = F, B$) is given in units of the Boltzmann constant k_B as

$$S_\alpha^{\mathrm{PDM}} = -\sum_j N_j [p_j \ln\ p_j \pm (1 \mp p_j)\ln(1 \mp p_j)], \tag{28}$$

where $p_j = n_j$ are the quasiparticle occupation numbers ($\alpha = F$) or phonon occupation numbers $p_j = \nu_j$ ($\alpha = B$), the upper (lower) sign is for quasiparticles (phonons), and $N_j = 2j + 1$ and 1 are for $\alpha = F$ and B, respectively. For $\alpha = F$, the index j denotes the single-particle energy level, which corresponds to the orbital angular momentum j, whereas, for $\alpha = B$, it corresponds to that of the GDR phonon. Because the quasiparticle (single-particle) damping is negligible for heavy nuclei [16], it is neglected in the present calculations of entropy S_F for the sake of simplicity by assuming $n_j = n_j^{\mathrm{FD}}$ from Eq. (11). With regard to the phonon occupation number for the GDR, it is approximated with the Bose-Einstein distribution $\nu_{\mathrm{GDR}} \simeq \nu_{\mathrm{GDR}}^B = [\exp(E_{\mathrm{GDR}}/T) - 1]^{-1}$ in the present calculations. This gives the upper bound for the entropy, hence, the lowest bound for the ratio η/s, estimated within the PDM. Indeed, the phonon occupation number ν_q, which includes the phonon damping, is given by Eq. (2.34) of Ref. [16]. For the GDR ($q = \mathrm{GDR}$), it is the Bose-Einstein distribution $\nu_{\mathrm{GDR}}^B = [\exp(E_{\mathrm{GDR}}/T) - 1]^{-1}$, smoothed with a Breit-Wigner kernel, whose width is equal to the GDR width, that is, $\nu_{\mathrm{GDR}} < \nu_{\mathrm{GDR}}^B$. Given $E_{\mathrm{GDR}} \gg T$, it turns out, however, that $S_B \ll S_F$ so that, in all the cases considered here, one has $S \simeq S_F$. For example, for ^{120}Sn, with $E_{\mathrm{GDR}} \simeq 15.5$ MeV and FWHM around 14 MeV at $T = 5$ MeV [15], one finds $\nu_{\mathrm{GDR}}^B \simeq 0.009$, which gives a negligible value 0.051 for S_B as compared to $S_F \simeq 109$ (in units of k_B).

The Fermi-gas formula for the entropy is

$$S^{\mathrm{FG}} = 2aT. \tag{29}$$

This formula is used in the FLDM and the analysis of experimental data. The level-density parameter $a = A/K$ with K varying from 8 to $13 \sim 14$ when A goes from the mass region of heavy nuclei to that of light ones. At $T \neq 0$, the level density also depends on T [14,18,45,46]. The experimental temperature, the width, and the energy of the GDR were deduced by using the temperature-dependent parametrization of the density parameter $a(T)$ shown as the dashed lines in the left and right panels of Fig. 4 of Ref. [10] for ^{120}Sn and ^{208}Pb, respectively. The same parametrization will be used here to calculate the empirical entropy density s from Eqs. (25) and (29) for tin and lead isotopes. For ^{63}Cu, the empirically adopted value $A/a = 8.8$ MeV is used for the temperature range where the GDR width was extracted [47,48]. As for S, which is used within the FLDM, the value of the level-density parameter a that best fits the microscopic and empirical entropies is adopted in the calculations. With regard to the entropy used for calculating η/s within the AM and pTSFM, although the precise one should be obtained from Eq. (26), the same entropy (density) as that used for the FLDM is adopted because only the liquid-drop version of these models is considered here.

IV. ANALYSIS OF NUMERICAL RESULTS

A. GDR width

Within the PDM, the GDR width obtained for ^{120}Sn, which includes the effect of thermal pairing in Ref. [17] is employed (the thick dotted line in Fig. 4(a) of Ref. [17]), whereas, for ^{208}Pb, the results of Ref. [15] are used (the solid line with diamonds in Fig. 1(b) of Ref. [15]). For ^{63}Cu, the effect of pairing on the GDR width is small, so it is not included in the GDR width calculations within the PDM. The values $F_1 = 0.332$ and $F_2 = 0.933$ MeV are chosen for this nucleus to reproduce a stable $E_{\mathrm{GDR}} \simeq 16$ to 17 MeV as T varies up to 5 MeV and the FWHM equal to around 7 MeV at $T < 0.5$ MeV in agreement with the experimental values of the ground-state GDR. The GDR widths predicted within the AM for ^{120}Sn and ^{208}Pb are read from the solid and dotted lines, respectively, of Fig. 5 of Ref. [18] because only the liquid-drop version of this model is considered here (for ^{120}Sn, shell corrections have a negligible effect on the GDR width as shown in Fig. 4 of Ref. [19]). As for the pTSFM and FLDM, the GDR width is calculated by using Eqs. (17) and (21), respectively.

Shown in Fig. 1 are the GDR widths predicted by the PDM, the AM, the pTSFM, and the FLDM as functions of temperature T in comparison with the experimental systematics [8–13,47,48], which are also collected in Ref. [49]. The PDM predictions best fit the experimental systematics for all three nuclei ^{63}Cu, ^{120}Sn, and ^{208}Pb. The AM (double dot-dashed lines) fails to describe the GDR width at low T for ^{120}Sn because thermal pairing was not included in the AM calculations, while it slightly overestimates the width for ^{208}Pb. (The AM prediction for GDR width in ^{63}Cu is not available.) The predictions by the pTSFM (dot-dashed lines) are qualitatively similar to those by the AM, although to achieve this agreement, the pTSFM needs to use $\Gamma(0) = 5$ MeV for ^{63}Cu and 3.8 MeV for ^{120}Sn, i.e., substantially smaller than the experimental values of around 7 and 4.9 MeV for ^{63}Cu and ^{120}Sn, respectively. This model also produces the width saturation similar to that predicted by the PDM, although for ^{63}Cu, the width obtained within the pTSFM at $T > 3$ MeV is noticeably smaller than that predicted by the PDM. The

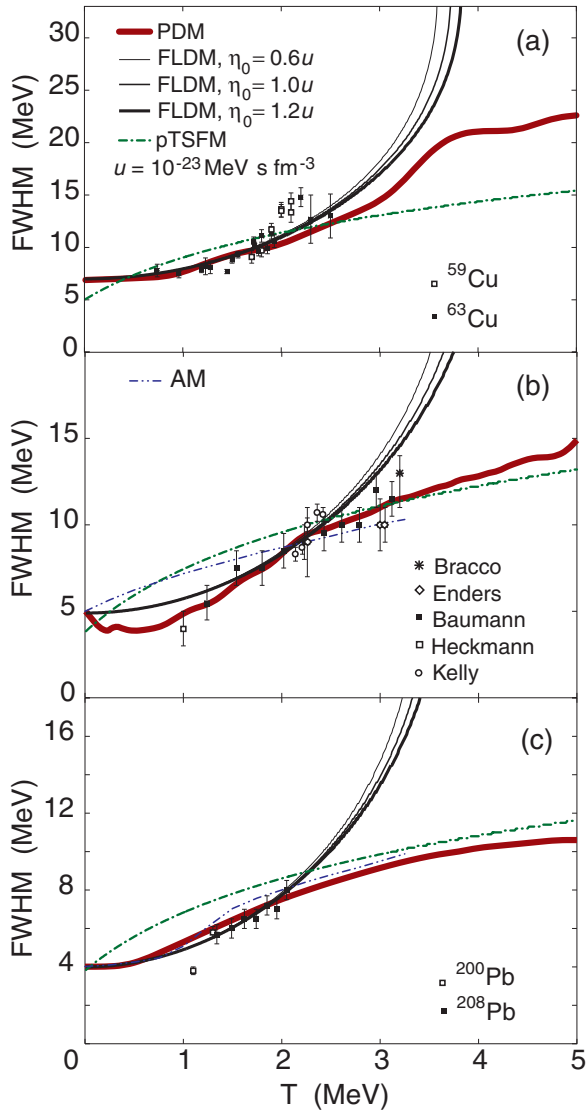

FIG. 1. (Color online) FWHM of the GDR as functions of T for (a) ^{63}Cu, (b) ^{120}Sn, and (c) ^{208}Pb in comparison with the experimental systematics for copper (Cu^{59} [47] and Cu^{63} [48]), tin (by Bracco *et al.* [8], Enders *et al.* [9], Baumann *et al.* [10], Heckmann *et al.* [11], and Kelly *et al.* [12]), and lead (Pb^{208} [10] and Pb^{200} [13]) regions. The notations for the theoretical curves are given in (a) and (b).

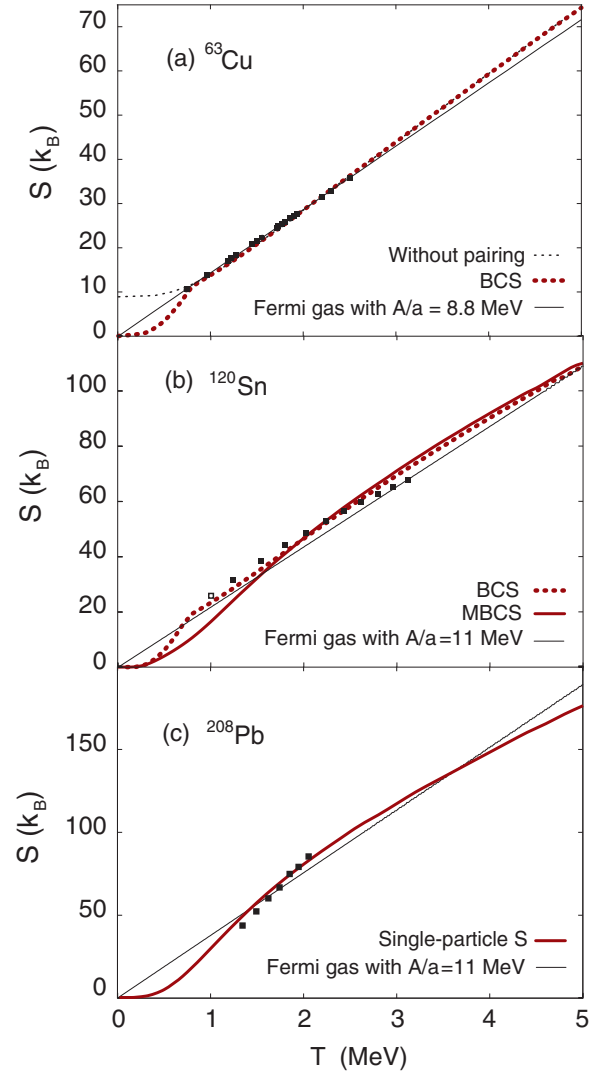

FIG. 2. (Color online) Entropies as functions of T for (a) ^{63}Cu, (b) ^{120}Sn, and (c) ^{208}Pb in comparison with the empirical values. The notations are the same as in Fig. 1.

widths obtained within the FLDM fit the data fairly well up to $T \simeq 2.5$ MeV. However, they do not saturate at high T but increase sharply with T and break down at $T_c < 4$ MeV. As has been mentioned previously in Sec. II B4, at $T > 2.5$ MeV, the dependence on $\eta(0)$ (ultimately α) starts to show up in the FLDM results for the GDR widths, which are 18.3, 17.5, and 17 MeV for $\eta_0 \equiv \eta(0) = 0.6$, 1.0, and $1.2u$, respectively, for ^{63}Cu at $T = 3$ MeV. The corresponding differences between the widths obtained by using these values of $\eta(0)$ for ^{120}Sn and ^{208}Pb are slightly smaller. The values of the critical temperature T_c, starting from which the FLDM width becomes imaginary, are 3.58, 3.72, and 3.83 MeV by using $\eta(0) = 0.6$, 1.0, and $1.2u$, respectively, for ^{63}Cu. For ^{120}Sn, these corresponding values for T_c are 3.77, 3.94, and 4.1 MeV, whereas, for ^{208}Pb, they are 3.42, 3.54, and 3.65 MeV, respectively. At these values of T_c, the ratio $\eta(T_c)/\eta(0)$ is smaller than 3.5, which is not much different from the estimation (23) (see later in Sec. IV C).

B. Entropy

Compared in Fig. 2 are the entropies obtained by using the microscopic expressions (27) and (28) and the empirical ones extracted from the Fermi-gas formula (29) by using the empirical values for the level-density parameter a discussed previously in Sec. III. The microscopic entropy includes pairing for open-shell nuclei. For ^{63}Cu, although pairing is not included in the calculation of the GDR width, the finite-temperature BCS pairing with blocking by the odd proton is taken into account for the entropy to ensure its vanishing value at low T [compare the thick dotted line obtained, which

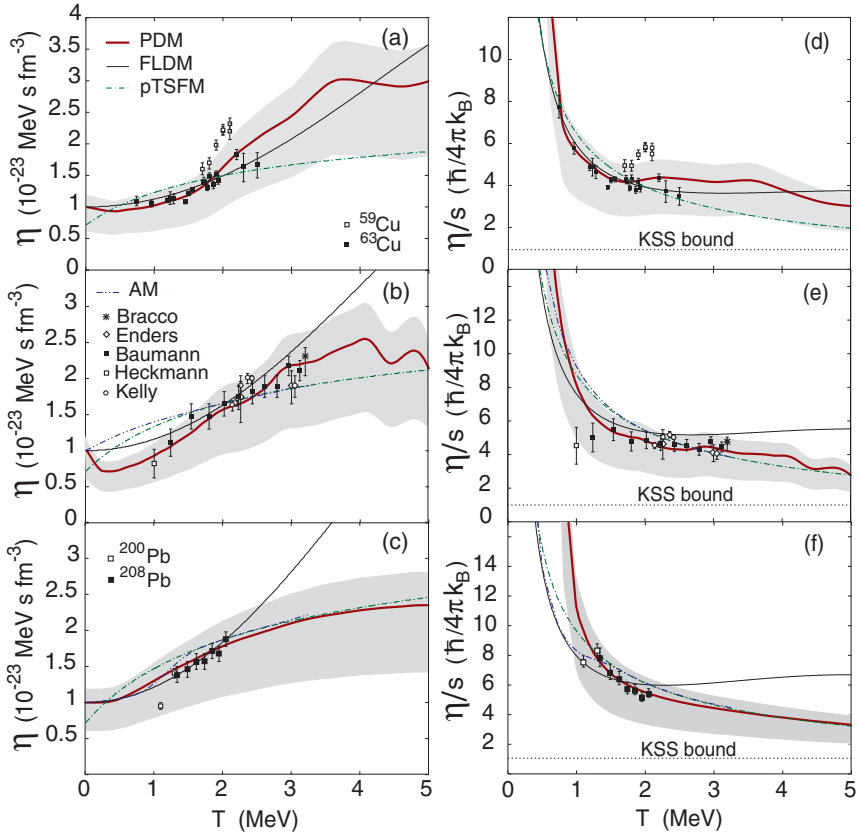

FIG. 3. (Color online) [(a)–(c)] Shear viscosity $\eta(T)$ and [(d)–(f)] ratio η/s as functions of T for nuclei in [(a) and (d)] copper, [(b) and (e)] tin, and [(c) and (f)] lead regions. The gray areas are the PDM predictions by using $0.6u \leqslant \eta(0) \leqslant 1.2u$. The same notations as in Fig. 1 are used to denote the empirical results, which are extracted by using the corresponding experimental widths and energies for the GDR in copper [47,48], tin [8–12], and lead [10,13] regions.

includes the BCS pairing, and the thin dotted line obtained without pairing in Fig. 2(a)]. For ^{120}Sn, the MBCS theory [40] is needed to reproduce the GDR width depletion at $T \leqslant 1$ MeV in this nucleus caused by the nonvanishing thermal pairing gap above the temperature of the BCS superfluid-normal phase transition [thick solid line in Fig. 1(b)], so the MBCS thermal pairing gap is also included in the calculation of the entropy. For the closed-shell nucleus ^{208}Pb, the quasiparticle entropy S_F in Eq. (28) becomes the single-particle entropy because of the absence of pairing. The good agreement between the results of microscopic calculations and the empirical extraction indicates that the level-density parameter for ^{63}Cu, within the temperature interval $0.7 < T < 2.5$ MeV, can be considered to be temperature-independent and equal to $a = 63/8.8 \simeq 7.16$ MeV^{-1}, whereas, for ^{120}Sn and ^{208}Pb, the level-density parameter varies significantly with T [10]. The Fermi-gas entropy $S^{\rm FG}$ (29) with a constant level-density parameter a best fits the microscopic and empirical results with $A/a =$ 8.8 MeV for ^{63}Cu, and 11 MeV for ^{120}Sn and ^{208}Pb.

C. Ratio η/s

1. Model-dependent predictions vs empirical results

The predictions for the shear viscosity η and the ratio η/s by the PDM, the FLDM, the AM, and the pTSFM for ^{63}Cu, ^{120}Sn, and ^{208}Pb are plotted as functions of T in Fig. 3 in comparison with the empirical results. The empirical values for η in Figs. 3(a)–3(c) are extracted from the experimental systematics for the GDR in copper, tin, and lead regions [8–13,47–49] making use of Eq. (6). The PDM predictions for η [thick solid lines and gray areas] are obtained from Eq. (6) by using the temperature-dependent GDR widths from Fig. 1 and $E_{\rm GDR}(T)$, which oscillates slightly around $E_{\rm GDR}(0)$ as T varies (see Fig. 4(b) of Ref. [17]). The predictions by the FLDM and AM are obtained by using the same resonance energy $\hbar\omega \equiv E_{\rm GDR} = E_{\rm GDR}(0)$ with $\eta(0) = 1u$ and $A/a = 8.8$ and 11 MeV because these values of A/a give the best fit to experimentally extracted entropies as shown in Fig. 2.[1]

In Fig. 3, it is seen that the predictions by the PDM have the best overall agreement with the empirical results for all three nuclei ^{63}Cu, ^{120}Sn, and ^{208}Pb. The PDM produces an increase in $\eta(T)$ with T up to 3–3.5 MeV and a saturation in $\eta(T)$ within (2 to 3)u at higher T [with $\eta(0) = 1u$]. The ratio η/s decreases sharply with increasing T up to $T \sim 1.5$ MeV, starting from which the decrease gradually slows down to reach (2 to 3) KSS units at $T = 5$ MeV. The FLDM has a similar trend as that of the PDM up to $T \sim 2$ to 3 MeV, but at higher T ($T > 3$ MeV for ^{120}Sn or 2 MeV for ^{208}Pb), it produces an increase in both η and η/s with T. At $T = 5$ MeV, the FLDM model predicts the ratio η/s within (3.7–6.5) KSS units, which are roughly 1.5 times—twice larger than the PDM predictions.

The AM and pTSFM show a similar trend for η and η/s. However, to obtain such similarity, $\eta(0)$ in the pTSFM

[1]In Ref. [5], the values $\hbar\omega = 20$ MeV and $\alpha = 9.2$, which correspond to the isoscalar mode, were used for Eqs. (18)–(20). The present paper extracts η/s from the GDR, so the use of $\hbar\omega = E_{\rm GDR}(0)$ and $\eta(0) = 1u$ is appropriate as it corresponds to $\alpha = 4.27$, close to the value 4.6 for the isovector mode within the FLDM [22].

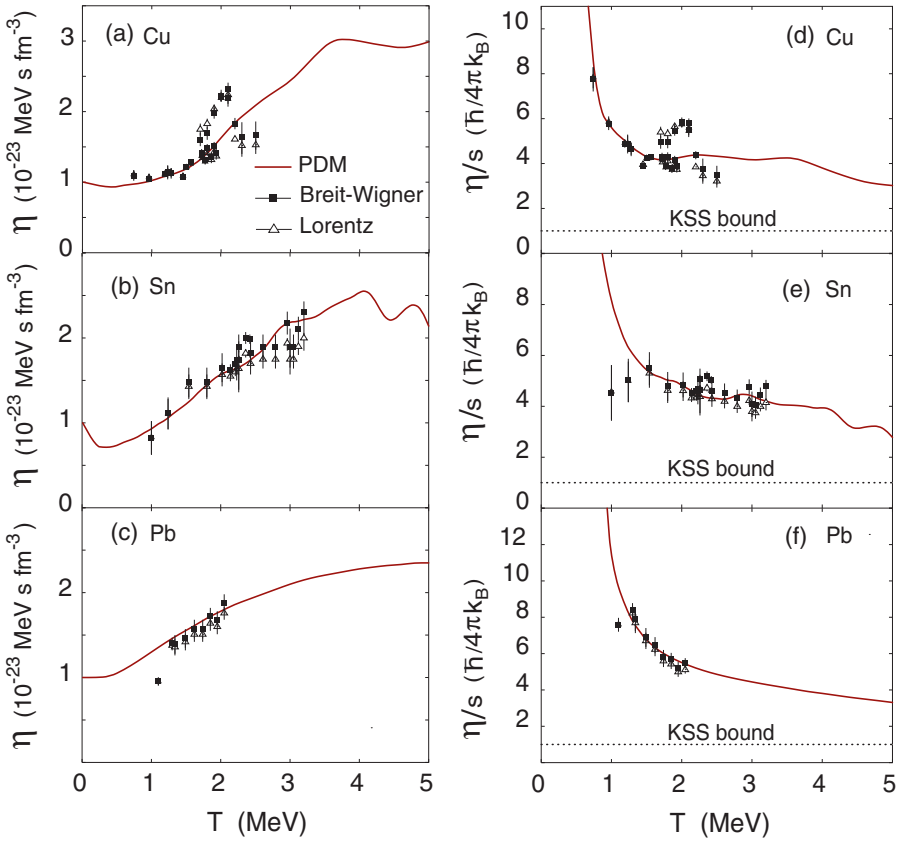

FIG. 4. (Color online) Shear viscosity $\eta(T)$ and ratio η/s as functions of T for nuclei in [(a) and (d)] copper, [(b) and (e)] tin, and [(c) and f)] lead regions. The solid boxes and open triangles with error bars denote the empirical results obtained by using Eqs. (6) and (24), respectively. The solid lines are the PDM predictions for ^{63}Cu, ^{120}Sn, and ^{208}Pb as in Fig. 3.

calculations has to be reduced to $0.72u$ instead of $1u$. They all overestimate η at $T < 1.5$ MeV. Because of the smaller $\eta(0)$ in use, the pTSFM predicts a much lower saturated value for η at high T for the lighter nucleus ^{63}Cu, and consequently, a smaller η/s, which amounts to around $2u$ at $T = 5$ MeV, i.e., comparable to the PDM's prediction by using $\eta(0) = 0.6u$.

The use of the Lorentz distribution instead of the Breit-Wigner one for the photoabsorption cross section does not cause a significant difference for η and, hence, η/s. As shown in Fig. 4, the use of Eq. (24) instead of Eq. (6) leads to some slight increase in η and η/s at low T and decrease in them at high T. Depending on the competition between $\Gamma(T)/\Gamma(0)$, which increases with T, and $\{E_{\rm GDR}(0)^2 - [\Gamma(0)/2]^2 + [\Gamma(T)/2]^2\}^{-2}$, which decreases as T increases, the values of η and η/s, obtained by using Eq. (24), can be larger or smaller than those predicted by Eq. (6). For example, Eq. (24) leads to slightly larger η and η/s for ^{59}Cu at $T < 2$ MeV but smaller values for these quantities for ^{63}Cu at $T > 2$ MeV. For ^{120}Sn and ^{208}Pb, the Lorentz distribution of the photoabsorption cross section produces slightly smaller η and η/s at high T.

2. *Model-independent assessment*

A model-independent estimation for the high-T limit of the ratio η/s can be inferred directly from Eqs. (6) and (28) under the assumption of GDR width saturation as follows. From the trend of the GDR width's increase, predicted by the PDM, the AM, and the pTSFM shown in Fig. 1, it can be assumed that, at the highest $T_{\rm max} \simeq 5$ to 6 MeV where the GDR can still exist, the GDR width $\Gamma(T)$ cannot exceed $\Gamma_{\rm max} \simeq 3\Gamma(0) \simeq 0.9E_{\rm GDR}(0)$ [7]. Because the GDR energy $E_{\rm GDR}(T)$ is stable against the variation of T, one can also set $E_{\rm GDR}(T) \simeq E_{\rm GDR}(0)$. By inserting these values into Eq. (6), the high-T limit of $\eta(T)$ is found as

$$\eta_{\rm max} \simeq 2.551 \times \eta(0). \tag{30}$$

The high-T limit of the entropy density s is obtained by noticing that $S_F \to 2\Omega \ln 2$ at $T \to \infty$ because $n_j \to 1/2$ where $\Omega = \sum_j (j + 1/2)$ for the spherical single-particle basis or sum of all doubly degenerate levels for the deformed basis. The particle-number conservation requires that $A = \Omega$ since all single-particle occupation numbers are equal to $1/2$. This leads to the following high-T limit of entropy density s (25):

$$s_{\rm max} = 2\rho \ln 2 \simeq 0.222(k_B). \tag{31}$$

Dividing the right-hand side of Eq. (30) with that of Eq. (31) yields the high-T limit (or lowest bound) for η/s in finite nuclei,

$$\left(\frac{\eta}{s}\right)_{\rm min} \simeq 2.2^{+0.4}_{-0.9}\ \text{(KSS units)}, \tag{32}$$

by using the empirical values for $\eta(0) = 1.0^{+0.2}_{-0.4}u$ [7,26].

To ensure the validity of this result, an alternative estimation is carried out by using the Fermi-gas entropy without assuming a width saturation [12]. From Eq. (6), it follows that the ratio $\eta(T)/s$ is not smaller than the KSS bound (1) only if the GDR

width $\Gamma(T)$ takes the values between $\Gamma_1 \leqslant \Gamma \leqslant \Gamma_2$, where

$$\Gamma_{1,2} = \eta(0)\frac{4E_{\rm GDR}(0)^2 + \Gamma(0)^2}{2sK\Gamma(0)} \times \left\{1 \pm \sqrt{1 - \left[\frac{4sK\Gamma(0)E_{\rm GDR}(T)}{\eta(0)(4E_{\rm GDR}(0)^2 + \Gamma(0)^2)}\right]^2}\right\}, \quad K = \frac{\hbar}{4\pi k_B}. \tag{33}$$

By inserting the entropy density (25) with S given by the Fermi-gas formula (29) into Eq. (33), where the lower and upper bounds for A/a are taken equal to 8 and 13 (MeV), respectively, for finite hot nuclei [40,46], one finds for $\eta(0) = 1.0u$ that, at $T = 6$ MeV, the GDR width Γ should be confined within the intervals $1.3 \leqslant \Gamma/\Gamma_0 \leqslant 34.8$ for $A/a = 8$ MeV and $0.8 \leqslant \Gamma/\Gamma_0 < 58$ for $A/a = 13$ MeV. The values for η/s, found at the middle of these intervals with $\Gamma/\Gamma_0 \simeq 18$ and 29.4, amount to $\eta/s \simeq 1.76$ KSS units for $A/a = 8$ MeV and 1.9 KSS units for $A/a = 14$ MeV. By including the error bars produced by the lower and upper values of $\eta(0)$ above, one finds

$$\frac{\eta}{s} \simeq 1.79^{+0.04}_{-0.34} \quad \text{and} \quad 1.9^{+0.03}_{-0.15}\ \text{(KSS units)} \tag{34}$$

for $A/a = 8$ and 14 MeV, respectively. The limit (34) turns out to be within the high-T limit (32).

V. CONCLUSIONS

In the present paper, by using the Kubo relation and the FDT, the shear viscosity η and the ratio η/s have been extracted from the experimental systematics for the GDR widths in copper, tin, and lead regions at $T \neq 0$ and have been compared with the theoretical predictions by four independent theoretical models. The calculations adopt the value $\eta(0) = 1.0^{+0.2}_{-0.4} \times u$ ($u = 10^{-23}$ MeV s fm^{-3}) as a parameter, which has been extracted by fitting the giant resonances at $T = 0$ [7] and fission data [26]. The analysis of numerical calculations shows that the shear viscosity η increases between (0.5 and 2.5)u with increasing T from 0.5 up to $T \simeq 3$–3.5 MeV for $\eta(0) = 1u$. At higher T, the PDM, the AM, and the pTSFM predict a saturation, or, at least, a very slow increase in η, whereas, the FLDM show a continuously strong increase in η with T. At $T = 5$ MeV, the PDM estimates η between around (1.3 and 3.5)u.

All theoretical models predict a decrease in the ratio η/s with increasing T up to $T \simeq 2.5$ MeV. At higher T, the PDM, the AM, and the pTSFM show a continuous decrease in η/s, whereas, the FLDM predicts an increase in η/s with increasing T. The PDM best fits the empirical values for η/s extracted at $0.7 \leqslant T \leqslant 3.2$ MeV for all three nuclei, ^{63}Cu, ^{120}Sn, and ^{208}Pb. At $T = 5$ MeV, the values of η/s, predicted by the PDM, reach $3^{+0.63}_{-1.2}$, $2.8^{+0.5}_{-1.1}$, $3.3^{+0.7}_{-1.3}$ KSS units for ^{63}Cu, ^{120}Sn, and ^{208}Pb, respectively. By combining these results with the model-independent estimation for the high-T limit of η/s, which is $2.2^{+0.4}_{-0.9}$ KSS units, one can conclude that the value of η/s for medium and heavy nuclei at $T = 5$ MeV is in between 1.3 and 4.0 KSS units, which is about three to five times smaller (and of much less uncertainty) than the value between 4 and 19 KSS units predicted by the FLDM for heavy nuclei where the same lower value $\eta(0) = 0.6u$ was used. By using the same upper value $\eta(0) = 2.5u$ as in Ref. [5], instead of $\eta(0) = 1.2u$, this interval for η/s becomes (1.3–8.3) KSS units, whose uncertainty of 7 KSS units is still smaller than that predicted by the FLDM (15 KSS units). This estimation also indicates that nucleons inside a hot nucleus at $T = 5$ MeV have nearly the same ratio η/s as that of QGP, around $2 \sim 3$ KSS units, at $T > 170$ MeV discovered at RHIC and LHC.

ACKNOWLEDGMENTS

The numerical calculations were carried out by using the FORTRAN IMSL Library by Visual Numerics on the RIKEN Integrated Cluster of Clusters (RICC) system. Thanks are due to G. F. Bertsch and P. Danielewicz for stimulating discussions as well as to N. Quang Hung for assistance with numerical calculations.

[1] (PHENIX Collaboration), K. Adcox *et al.*, Nucl. Phys. A **757**, 184 (2005); B. B. Back *et al.*, *ibid.* **757**, 28 (2005); (BRAHMS Collaboration), J. Arsene *et al.*, *ibid.* **757**, 1 (2005); (STAR Collaboration), J. Adams *et al.*, *ibid.* **757**, 102 (2005).
[2] K. Arnold *et al.* (ALICE Collaboration), Phys. Rev. Lett. **105**, 252302 (2010); G. Aad *et al.* (ATLAS Collaboration), *ibid.* **105**, 252303 (2010).
[3] P. K. Kovtun, D. T. Son, and A. O. Starinets, Phys. Rev. Lett. **94**, 111601 (2005).
[4] T. Schäffer and D. Teaney, Rep. Prog. Phys. **72**, 126001 (2009); E. Shuryak, Phys. **3**, 105 (2010).
[5] N. Auerbach and S. Shlomo, Phys. Rev. Lett. **103**, 172501 (2009).
[6] V. M. Kolomietz and S. Shlomo, Phys. Rep. **390**, 133 (2004).
[7] N. Auerbach and A. Yeverechyahu, Ann. Phys. (NY) **95**, 35 (1975).
[8] A. Bracco *et al.*, Phys. Rev. Lett. **62**, 2080 (1989).
[9] G. Enders *et al.*, Phys. Rev. Lett. **69**, 249 (1992).
[10] T. Baumann *et al.*, Nucl. Phys. A **635**, 428 (1998).
[11] P. Heckmann *et al.*, Phys. Lett. B **555**, 43 (2003).
[12] M. P. Kelly, K. A. Snover, J. P. S. van Schagen, M. Kicińska-Habior, and Z. Trznadel, Phys. Rev. Lett. **82**, 3404 (1999).
[13] D. R. Chakrabarty, M. Thoennessen, N. Alamanos, and P. Paul, and S. Sen, Phys. Rev. Lett. **58**, 1092 (1987).
[14] S. Shlomo and J. B. Natowitz, Phys. Rev. C **44**, 2878 (1991).
[15] N. D. Dang and A. Arima, Phys. Rev. Lett. **80**, 4145 (1998).
[16] N. Dinh Dang and A. Arima, Nucl. Phys. A **636**, 427 (1998).
[17] N. D. Dang and A. Arima, Phys. Rev. C **68**, 044303 (2003).
[18] W. E. Ormand, P. F. Bortignon, R. A. Broglia, and A. Bracco, Nucl. Phys. A **614**, 217 (1997).
[19] D. Kusnezov, Y. Alhassid, and K. A. Snover, Phys. Rev. Lett. **81**, 542 (1998).

[20] H. Lamb, *Hydrodynamics*, 6th ed. (Cambridge University Press, Cambridge, UK, 1994).
[21] W. J. Swiatecki and S. Bjotnholm, Phys. Rep. **4**, 325 (1972).
[22] V. M. Kolomietz, V. A. Plujko, and S. Shlomo, Phys. Rev. C **54**, 3014 (1996).
[23] C. Fiolhais, Ann. Phys. **171**, 186 (1986).
[24] J. Blocki, Y. Boneh, J. R. Nix, J. Randrup, M. Robel, A. J. Sierk, and W. J. Swiatucki, Ann. Phys. **113**, 330 (1978).
[25] J. R. Nix and A. J. Sierk, Phys. Rev. C **21**, 396 (1980).
[26] K. T. R. Davies, A. J. Sierk, and J. R. Nix, Phys. Rev. C **13**, 2385 (1976).
[27] K. T. R. Davies, R. A. Managan, J. R. Nix, and A. J. Sierk, Phys. Rev. C **16**, 1890 (1977).
[28] A. J. Sierk and J. R. Nix, Phys. Rev. C **21**, 982 (1980).
[29] D. V. Vanin, P. N. Nadtochy, G. I. Kosenko, and G. D. Adeev, Phys. At. Nucl. **63**, 1865 (2000).
[30] P. Fröbrich, I. I. Gontchar, and N. D. Mavlitov, Nucl. Phys. A **556**, 281 (1993).
[31] R. Kubo, H. Hasegawa, and N. Hashitsume, J. Phys. Soc. Jpn. **14**, 56 (1959).
[32] D. N. Zubarev, Sov. Phys. Usp. **3**, 320 (1960) [Usp. Fiz. Nauk. **71**, 71 (1960)].
[33] M. S. Green, J. Chem. Phys. **22**, 398 (1954); R. Kubo, J. Phys. Soc. Jpn. **12**, 570 (1957).
[34] S. R. Das, G. H. Gibbons, and S. D. Mathur, Phys. Rev. Lett. **78**, 417 (1997).
[35] A. Barnett, D. Cohen, and E. J. Heller, J. Phys. A **34**, 413 (2001).
[36] G. Breit and E. Wigner, Phys. Rev. **49**, 519 (1936).
[37] M. Brack and P. Quentin, Phys. Lett. B **52**, 159 (1974); P. Bonche, S. Levit, and D. Vautherin, Nucl. Phys. A **436**, 265 (1985).
[38] H. Sagawa and G. F. Bertsch, Phys. Lett. B **146**, 138 (1984); N. Dinh Dang, J. Phys. G **11**, L125 (1985); P. F. Bortignon, R. A. Broglia, G. F. Bertsch, and J. Pacheco, Nucl. Phys. A **460**, 149 (1986); N. D. Dang, *ibid.* **504**, 143 (1989).
[39] L. G. Moretto, Phys. Lett. B **40**, 1 (1972).
[40] N. D. Dang and A. Arima, Phys. Rev. C **68**, 014318 (2003).
[41] N. Dinh Dang and N. Quang Hung, Phys. Rev. C **77**, 064315 (2008).
[42] D. J. Dean, K. Langanke, H. A. Nam, and W. Nazarewicz, Phys. Rev. Lett. **105**, 212504 (2010).
[43] B. L. Berman and S. C. Fultz, Rev. Mod. Phys. **47**, 713 (1975).
[44] M. Danos and W. Greiner, Phys. Rev. **138**, B876 (1965).
[45] W. Reisdorf, Z. Phys. A **300**, 227 (1981); W. Reisdorf and J. Törke, *ibid.* **302**, 183 (1981).
[46] K. Hagen *et al.*, Nucl. Phys. A **486**, 429 (1988); M. Gonin *et al.*, Phys. Rev. C **42**, 2125 (1990); B. J. Fineman, K.-T. Brinkmann, A. L. Caraley, N. Gan, R. L. McGrath, and J. Velkovska, *ibid.* **50**, 1991 (1994).
[47] Z. M. Drebi, K. A. Snover, A. W. Charlop, M. S. Kaplan, D. P. Wells, D. Ye, and Y. Alhassid, Phys. Rev. C **52**, 578 (1995).
[48] M. Kicińska-Habior *et al.*, Phys. Rev. C **36**, 612 (1987); E. F. Garman, K. A. Snover, S. H. Chew, S. K. B. Hesmondhalgh, W. N. Catford, and P. M. Walker, *ibid.* **28**, 2554 (1983).
[49] A. Schiller and M. Thoennessen, At. Data Nucl. Data Tables **93**, 548 (2007).